

Synergistic Interaction within Bifunctional Ruthenium Nanoparticle/SILP Catalysts for the Selective Hydrodeoxygenation of Phenols

Kylie L. Luska, Pedro Migowski, Sami El Sayed, and Walter Leitner*

Abstract: Ruthenium nanoparticles immobilized on acid-functionalized supported ionic liquid phases (RuNPs@SILPs) act as efficient bifunctional catalysts in the hydrodeoxygenation of phenolic substrates under batch and continuous flow conditions. A synergistic interaction between the metal sites and acid groups within the bifunctional catalyst leads to enhanced catalytic activities for the overall transformation as compared to the individual steps catalyzed by the separate catalytic functionalities.

Lignocellulosic materials are a potential renewable feedstock for the manufacture of chemicals and fuels in the chemical industry as they represent a non-edible resource that can be produced in short timeframes and on large scales.^[1] Much progress has been made toward the production of various classes of value-added products (for example, ethers, alcohols, and alkanes) from pentose- and hexose-derived platform chemicals;^[2–4] however, valorization of the lignin fraction remains a significant challenge.^[5] As such, a significant amount of research has focused on the development of homogeneous^[6] and heterogeneous-based^[7] catalytic strategies towards the production of chemicals and fuels from lignin.

One strategy towards the utilization of lignin involves depolymerization into oligomeric and monomeric aromatic components (primarily substituted phenols), followed by deoxygenation of the phenolic intermediates to arenes and cycloalkanes.^[8] Although high yields of monomeric phenols can be obtained by the depolymerization of lignin using pyrolysis, hydrogenolysis, or hydrolysis,^[9] the subsequent hydrodeoxygenation of these substrates using conventional CoMo and NiMo sulfide catalysts suffers from sulfur contamination of the product and catalyst deactivation.^[8] Novel deoxygenation catalysts have been developed in which the combination of an acid (for example, a Lewis or Brønsted acid) and a metal catalyst (such as commercial heterogeneous catalysts or metal nanoparticles), defined herein as a bifunctional catalyst, has shown significant potential for the hydrodeoxygenation of phenols.^[10] This transformation comprises

a network of metal- and acid-catalyzed reactions, in which the removal of oxygenated moieties involves the acid and metal components working independently (for example, metal-catalyzed hydrogenation coupled with acid-catalyzed dehydration) and/or cooperatively (for example, hydrogenolysis catalyzed by both metal and acid components of the bifunctional catalyst). Despite the growing number of bifunctional catalysts, a detailed analysis of the individual and combined action of the two catalytic moieties to control the reaction network is seldom available making the rational design of such materials still challenging.

In our present work, we describe the application of a bifunctional catalyst composed of nanoparticles immobilized on a supported ionic liquid phase (NP@SILP) in the hydrodeoxygenation of phenols. A synergistic relationship between the metal and acid components can be tuned through the molecular, bottom-up synthesis of the materials to provide an enhanced catalytic performance for the overall transformation as compared to the individual steps catalyzed by the separate catalytic functionalities.

The general design of these bifunctional metal NP@SILP catalysts is based on a molecular approach to assemble the individual components onto solid materials in a flexible and controlled manner (Figure 1).^[11] The support is synthesized by

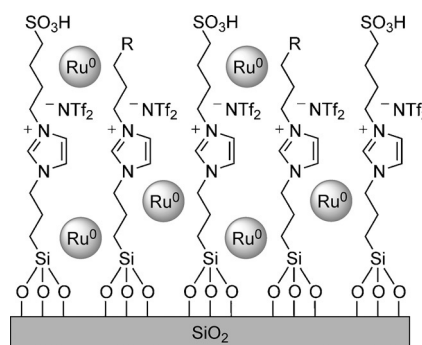


Figure 1. Bifunctional catalysts, composed of Ru nanoparticles and an acid-functionalized supported ionic liquid phase (RuNPs@SILP), employed for the hydrodeoxygenation of phenolic substrates. R = CH₂SO₃H (IL 1), R = CH₃ (IL 2).

tethering functionalized and/or nonfunctionalized imidazolium-based ionic liquids (ILs) onto silica,^[12] in which the degree of functionality on the support can be tuned through the ratio of functionalized to nonfunctionalized imidazolium units.^[3b] Even though these surface layers are of course no longer true “liquid phases”, the materials are generally referred to as supported ionic liquid phases (SILPs).^[13] The

[*] Dr. K. L. Luska, Dr. P. Migowski, S. El Sayed, Prof. Dr. W. Leitner
Institut für Technische und Makromolekulare Chemie (ITMC)
RWTH Aachen University
Worringerweg 1, 52074 Aachen (Germany)
E-mail: leitner@itmc.rwth-aachen.de

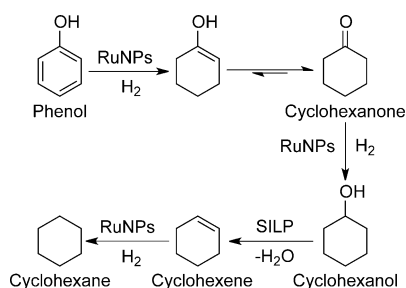
Prof. Dr. W. Leitner
Max-Planck-Institut für Kohlenforschung
45470 Mülheim an der Ruhr (Germany)

Supporting information for this article is available on the WWW under <http://dx.doi.org/10.1002/anie.201508513>.

IL-like structure of the surface layer provides a stabilizing environment for metal nanoparticles^[14] formed from organometallic precursors in a controlled chemical reaction. This approach combines the molecular diversity of the IL-like structures with the catalytic activity of metal nanoparticles.^[11] For deoxygenation processes required in selective biomass conversion, the combination of acidic functionalities with Ru metal NPs is particularly attractive.^[3,4,10c,15]

Acidic SILPs were synthesized according to a modified literature procedure^[3b] and involved the condensation of a sulfonic acid functionalized IL [1-(4-sulfobutyl)-3-(3-triethoxysilylpropyl)-imidazolium]NTf₂ (IL **1**), and a nonfunctionalized IL [1-butyl-3-(3-triethoxysilylpropyl)imidazolium]NTf₂ (IL **2**), with dehydroxylated SiO₂. The combination of an acid-functionalized IL **1** and a nonfunctionalized IL **2** allowed for control of the quantity of grafted sulfonic acid moieties (defined as SILP acidity or acid loading = IL **1**/[IL **1** + IL **2**]; see Table S1 in the Supporting Information). RuNPs were synthesized and immobilized onto SILPs (RuNPs@SILP) by means of wet impregnation of the SILP with a solution of [Ru(2-methylallyl)₂cod] (cod = 1,5-cyclooctadiene), followed by reduction of the dried SILP under an atmosphere of H₂. Characterization of the RuNPs@SILPs using scanning transmission electron microscopy (STEM) showed the production of small and well-dispersed RuNPs (1.6–1.9 nm). A Ru loading of 0.23 wt % was determined for the bifunctional catalysts using inductively coupled plasma atomic adsorption spectroscopy (ICP-AAS; see the Supporting Information for full synthetic and characterization details).

RuNPs@SILPs were investigated as bifunctional catalysts for the hydrodeoxygenation of phenol, where the reaction pathway involves a series of metal- and acid-catalyzed reactions as outlined in Scheme 1. Aromatic hydrogenation



Scheme 1. Reaction pathway for the hydrodeoxygenation of phenol catalyzed by RuNPs@SILP.

of phenol is catalyzed by RuNPs to cyclohexanone and further to cyclohexanol. Dehydration of cyclohexanol by the acidic SILP yields cyclohexene, and subsequent hydrogenation involving RuNPs provides the saturated product cyclohexane. Integration of the RuNPs onto a sulfonic acid functionalized SILP to form a bifunctional catalyst was anticipated to allow for this reaction cascade to be carried out in a single-pot reaction and under continuous flow conditions.

RuNPs@SILPs were first investigated for the hydrodeoxygenation of phenol under batch conditions, in which a series of bifunctional catalysts were examined (Table 1).

Table 1: Hydrodeoxygenation of phenol using Ru NPs@SILP.^[a]

Entry	Catalyst	Conversion [%]	Product Yield [%] ^[b]			
			Ketone	Alcohol	Alkene	Alkane
1	Ru NPs@SILP-0.33	93	33	51	0	9
2	Ru NPs@SILP-0.66	> 99	3	73	0	24
3	Ru NPs@SILP-1.00	> 99	0	59	0	41
4 ^[c]	Ru NPs@SILP-1.00	> 99	0	5	0	95
5 ^[d]	Ru NPs@IL	62	19	11	0	32

[a] Reaction conditions: Ru NPs@SILP (75 mg, 0.0024 mmol Ru), substrate (6.0 mmol, 2500 equiv), decalin (1 mL), H₂ (120 bar), 2 h, 150 °C. [b] Determined by GC using hexadecane as an internal standard.

[c] Substrate (2.4 mmol, 1000 equiv), 16 h, 175 °C. [d] RuNPs stabilized in [1-butyl-3-(4-sulfobutyl)imidazolium]NTf₂: [Ru] (0.0024 mmol Ru), IL (0.051 mmol).

The acid loading of the SILP was varied between 0.33 and 1.00 and was shown to influence both the catalytic activity and selectivity of the bifunctional catalysts. Under standard conditions (2500 equiv phenol, 150 °C, 120 bar H₂, 2 h), RuNPs@SILP-0.33 did not achieve full phenol conversion (Table 1, entry 1), whereas an increased SILP acidity provided

quantitative conversions of phenol for RuNPs@SILP-0.66 and RuNPs@SILP-1.00 (Table 1, entries 2 and 3). In terms of the catalytic selectivity, higher acid loadings of the SILP shifted the product selectivity away from the alcohol and more toward the deoxygenated product cyclohexane (Table 1, entries 1–3). A yield of more than 95 % of cyclohexane was achieved using RuNPs@SILP-1.00 at 175 °C (Table 1, entry 4). The hydrodeoxygenation of phenol was also performed using an unsupported bifunctional catalyst in which RuNPs were immobilized in a homogeneous sulfonic acid functionalized IL [1-butyl-3-(4-sulfobutyl)imidazolium]NTf₂ (RuNPs@IL).^[3a] The catalytic activity of RuNPs@IL was significantly decreased in comparison to SILP-based bifunctional catalysts (Table 1, entry 5) because the colloidal RuNPs were unstable under catalytic conditions leading to precipitation of bulk metal from the IL phase during the reaction (Figure S6). Thus, the immobilization of IL **1** onto SiO₂ provided improved NP stability, probably through the combination of electrosteric stabilization of the IL and steric protection provided by the inert support material.^[16]

The hydrodeoxygenation of phenol was investigated under continuous flow conditions using the most active bifunctional catalyst RuNPs@SILP-1.00. A solution of phenol (0.05 M in decalin) was passed over a cartridge packed with RuNPs@SILP-1.00 using a H-Cube Pro (a continuous flow reactor), where the influence of the reaction temperature, substrate flow, and H₂ flow on the catalytic activity and selectivity was investigated (Table S3). At a substrate flow rate of 0.3 mL min⁻¹ (residence time = 2.00 min),

a reaction temperature of 135 °C or more was required to achieve quantitative conversion of phenol. Under these conditions, an increased temperature (150 °C) provided higher quantities of the deoxygenated products cyclohexene and cyclohexane (> 99 % conversion, 56 % deoxygenation product yield). Increased substrate flows led to full conversion of phenol between 0.3 and 0.9 mL min⁻¹ (residence time = 2.00 and 0.67 min, respectively). However, under these conditions the alkane yield decreased from 52 % to 28 % whereas the alkene yield doubled from 4 % to 8 %. The H₂ flow rate did not have a significant influence on the catalytic behavior of the bifunctional catalyst.

From this parameter screening, conditions were selected that provided a mixture of hydrogenation and deoxygenation products to evaluate the long-term behavior of Ru NPs@SILP-1.00 (*T* = 150 °C, substrate flow rate = 0.3 mL min⁻¹, H₂ flow rate = 60 NmL min⁻¹, *t* = 4 h; Figure 2, Table S4). The hydrogenation of phenol catalyzed by Ru NPs occurred rapidly under continuous flow conditions to give quantitative conversion over 240 minutes time-on-stream. A largely constant amount of the primary hydrogenation products cyclohexanone (6–9 %) and cyclohexanol (34–39 %) was detected throughout the reaction. The total yield of deoxygenated products was also consistent (55–60 %) over the course of the reaction. The composition of the alkene/alkane mixture, however, changed during time-on-stream as the yield of cyclohexene increased from 6 % to 30 %, while concomitantly that of cyclohexane decreased from 51 % to 30 %.

Analysis of Ru NP@SILP-1.00 after catalysis did not show significant growth or aggregation of the Ru NPs by STEM (1.80 ± 0.3 nm; Figure S5), ICP measurements did not evidence any leaching of Ru or the IL, and changes to the textural properties were not detected by BET surface-area analysis (Table S5). As the Ru NP@SILP bifunctional catalysts appear to be quite stable materials under continuous flow conditions, we set out to determine the activity of each of the individual reaction steps to identify the reason for a change in the product selectivity. Using two separate materials, one containing the acid moiety and one comprising the metal functionality, kinetic parameters for the elementary reactions involved in the reaction sequence leading to hydrodeoxygenation of phenol were determined.

The reaction rates for the elementary reactions involved in the phenol hydrodeoxygenation pathway were determined for SILP-based catalysts, where pseudo zero-order kinetics were detected during the initial stages of the reactions (Table 2; Figure S2). First, the elementary reactions were investigated using the individual metal- (Ru NPs@SILP-0.00) and acid-based components (SILP-

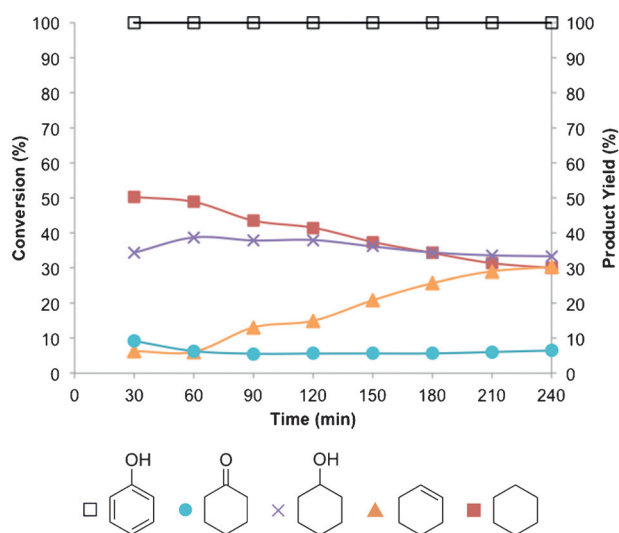


Figure 2. Hydrodeoxygenation of phenol (0.05 M in decalin, 0.3 mL min⁻¹) using Ru NPs@SILP-1.00 (550 mg, 0.0176 mmol Ru) under continuous flow conditions at 150 °C and 80 bar H₂ (gas flow rate under standard conditions = 60 NmL min⁻¹).

1.00), in which reaction rates (*r*) were derived from the consumption of the substrates. The hydrogenation of phenol ($-r_{\text{phenol}}$) to the primary hydrogenation products cyclohexanone and cyclohexanol catalyzed by Ru NPs@SILP-0.00 had a reaction rate of 1.74 M h⁻¹ (Table 2, Entry 1a), in which negligible quantities of cyclohexane (< 1 %) were produced in the absence of an acid catalyst. Dehydration of cyclohexanol ($-r_{\text{alcohol}}$) using SILP-1.00 provided cyclohexene with a rate of 0.02 M h⁻¹ and the subsequent hydrogenation of cyclohexene ($-r_{\text{alkene}}$) catalyzed by Ru NPs@SILP-0.00 yielded cyclohexane at a rate of 20.7 M h⁻¹ (Table 2, Entries 1b and 1c). From these kinetic experiments, the rate-limiting elementary reaction was determined to be the acid-catalyzed dehydration of cyclohexanol, which was about 87 and 1035 times slower than

Table 2: Reaction rates for the hydrodeoxygenation of phenol using SILP-based catalysts.^[a]

Reaction	Catalyst	Reaction rates [M h ⁻¹] ^[b]
1) Elementary Reactions:		
a) Phenol hydrogenation	Ru NPs@SILP-0.00	$-r_{\text{phenol}} = 1.74$
b) Cyclohexanol dehydration	SILP-1.00	$-r_{\text{alcohol}} = 0.02$
c) Cyclohexene hydrogenation	Ru NPs@SILP-0.00	$-r_{\text{alkene}} = 20.7$
2) Tandem/Integrated Reactions:		
a) Physical mixture	Ru NPs@SILP-0.00 + SILP-1.00	$-r_{\text{phenol}} = 0.73$ $+r_{\text{total}} = 0.07$
b) Bifunctional catalyst	Ru NPs@SILP-1.00	$-r_{\text{phenol}} = 1.62$ $+r_{\text{total}} = 0.47$

[a] Reaction conditions: Ru NPs@SILP (225 mg, 0.0072 mmol Ru), substrate (18.0 mmol, 2500 equiv), decalin (3 mL), H₂ (120 bar), 125 °C. [b] Determined by GC using hexadecane as an internal standard during the first 2 h of reaction.

the metal-catalyzed hydrogenation of phenol and cyclohexene, respectively. These results provided evidence on the behavior of the bifunctional catalyst under continuous flow conditions (Figure 2), in which changes in the product selectivity were likely caused by a decrease in the reaction rate of the slowest step in this transformation, that is, the dehydration of cyclohexanol. Due to the lack of back mixing under continuous flow conditions, a decreased cyclohexanol dehydration rate led to a shorter retention time of the intermediate cyclohexene for the subsequent hydrogenation to cyclohexane. As the catalyst materials were found to be quite stable under catalytic conditions, the reason for a decreased dehydration rate may result from the accumulation of water formed during the reaction within the catalyst bed.

Kinetic experiments were also performed for the tandem reaction employing a physical mixture of the individual metal- and acid-based catalysts, RuNPs@SILP-0.00 and SILP-1.00, and for the integrated reaction using the bifunctional catalyst RuNPs@SILP-1.00. The hydrodeoxygenation of phenol catalyzed by the physical mixture had a reaction rate of 0.73 m h^{-1} for the consumption of phenol, probably reflecting the dilution of the metal catalyst with unloaded support (Table 2, entry 2a). In comparison, the conversion of phenol catalyzed by RuNPs@SILP-1.00 had a reaction rate of 1.62 m h^{-1} (Table 2, entry 2b), which was more than twice the rate of the physical mixture and similar to the phenol hydrogenation in the absence of acid. Most significantly, the overall reaction rate towards the production of cyclohexane ($+r_{\text{total}}$) was significantly improved for the bifunctional catalyst, as the rate was almost seven times higher than that for the physical mixture (0.47 versus 0.07 m h^{-1} , respectively). These results show that immobilization of the metal and acid species within the RuNP@SILP bifunctional catalysts leads to a synergistic interaction between the two catalytic components. According to this data, the effect largely results from an increase of the dehydration rate which may be due to the fact that the substrate for this step is formed from the hydrogenation of phenol, in close proximity to the acidic site.

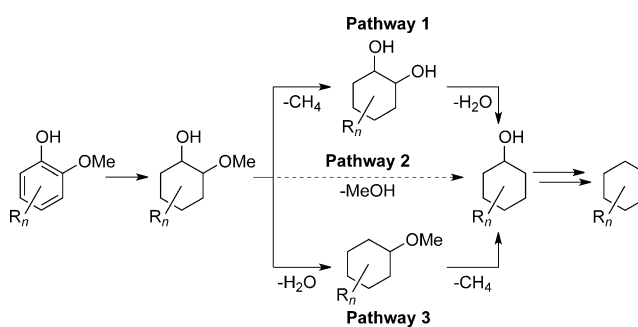
Next, the performance of the bifunctional catalyst in the hydrodeoxygenation of substituted phenolic substrates was investigated (Table 3). Alkyl substitution of phenol did not affect the reaction as quantitative hydrodeoxygenation of *p*-cresol (4-methylphenol) to methylcyclohexane was achieved at 175°C (Table 3, entry 1). The bifunctional catalysts also tolerated ether substitution of the phenolic ring as the deoxygenation of anisole (methoxybenzene) to cyclohexane was achieved in high yields (Table 3, entry 2). Deoxygenation of di- and trisubstituted phenols, guaiacol (2-methoxyphenol) and creosol (2-methoxy-4-methylphenol), was effectively catalyzed by RuNPs@SILP-1.00 leading to yields of more than 77% for the cyclohexane products (Table 3, entries 3 and 4). Thus, the close contact between the metal and acid sites within the RuNP@SILP bifunctional catalysts also facilitates the hydrogenolysis of ether moieties, wherein the deoxygenation of ether-substituted phenols involves a series of dehydration, hydrogenation, and hydrogenolysis reactions.

The reaction network for the deoxygenation of ether-substituted phenols catalyzed by RuNPs@SILP is outlined in

Table 3: Deoxygenation of phenolic derivatives using Ru NPs@SILP-1.00.^[a]

Entry	Substrate	Ether	Product Yield (%) ^[b]		
			Alcohol	Alkane	
1		—	—	0	> 99
2 ^[c]			21	3	76
3			14	1	81
4			18	4	77

[a] Reaction conditions: Ru NPs@SILP-1.00 (75 mg, 0.0024 mmol Ru), substrate (2.4 mmol, 1000 equiv), decalin (1 mL), H₂ (120 bar), 16 h, 175°C . [b] Conversion > 99%, determined by GC using hexadecane as an internal standard. [c] Substrate (1.2 mmol, 500 equiv).



Scheme 2. Reaction network for the deoxygenation of substituted phenols catalyzed by Ru NPs@SILP. Note: each reaction step requires the RuNP@SILP-1.00 catalyst and H₂ as reagents, which have been omitted here for clarity.

Scheme 2. Aromatic hydrogenation of the phenolic ring yields methoxycyclohexanols, which can be deoxygenated to cyclohexanol through three possible pathways: 1) hydrogenolysis of the methoxy group to produce 1,2-cyclohexanediols and subsequent dehydration/hydrogenation to cyclohexanols; 2) direct hydrogenolysis of the methoxy group to form cyclohexanols; and 3) dehydration/hydrogenation of the hydroxy group to yield methoxycyclohexanes and successive hydrogenolysis of the methoxy group to cyclohexanols. Dehydration/hydrogenation of the intermediate cyclohexanols allows for the complete deoxygenation to form cyclohexanes. GC analysis of the reactions mixtures allowed for a discrimination between the possible deoxygenation pathways (Table S2). For the deoxygenation of guaiacol (150°C , 120 bar H₂, 6 h), the major intermediates formed were 2-methoxycyclohexanol (25%) and cyclohexanol (27%), the minor species were 1,2-cyclohexanediol (4%) and methoxycyclohexane (4%), and MeOH was not produced. Comparable intermediates were formed during the deoxygenation of

creosol as 2-methoxy-4-methylcyclohexanol (31%) and 4-methylcyclohexanol (35%) were the predominate intermediates, while low concentrations of 4-methyl-1,2-cyclohexanediol (6%) and 1-methoxy-3-methylcyclohexane (3%) were formed. As such, RuNPs@SILP catalyzed the deoxygenation of substituted phenols through pathways 1 and 3 (Scheme 2) involving the hydrogenolysis of the methoxy group into an alcohol intermediate and methane, followed by the dehydration/hydrogenation of the hydroxy group (or vice versa). The direct hydrogenolysis of the methoxy group from the cyclohexane ring (pathway 2) was not a preferred deoxygenation route, as methanol was not formed during these reactions. Therefore, RuNP@SILP bifunctional catalysts operate through pathways 1 and 3 to achieve the deoxygenation of ether-substituted phenols. These competing pathways operate simultaneously and are the rate-determining step in this transformation.

In summary, the hydrodeoxygenation of phenolic substrates was achieved using bifunctional catalysts composed of ruthenium nanoparticles immobilized on an acid-functionalized supported ionic liquid phase. RuNPs@SILPs possessed high catalytic activities and selectivities for the hydrodeoxygenation of phenol to cyclohexene and cyclohexane under batch and continuous flow conditions, in which modulation of the SILP acidity allowed for control of the bifunctional catalyst properties. Kinetic determination of the elementary and tandem reaction rates involved in phenol hydrodeoxygenation was accomplished by using the individual metal- or acid-based catalytic materials, or by employing a physical mixture of the metal and acid components. In comparison, RuNPs@SILP-1.00 showed superior hydrogenation and deoxygenation activities resulting from intimate contact between the metal and acid components within the bifunctional catalyst. This cooperative effect provided active catalysts for the deoxygenation of ether-substituted phenols as model compounds for lignin cleavage products. The favored pathway for this reaction involved the hydrogenolysis of ether moieties to cyclohexanol intermediates and dehydration/hydrogenation of hydroxy groups to cycloalkane products. The possibility to control this synergistic interaction may have widespread implications within the field of biomass conversion, as bifunctional catalysis has been a popular strategy to find selective pathways in the complex networks of acid- and metal-catalyzed reactions involved in the deoxygenation of bio-based substrates.^[4] Further studies within our group will involve catalytic tests to determine whether RuNP@SILP catalysts provide enhanced deoxygenation rates for other classes of renewable feedstocks. Additionally, mechanistic investigations will be undertaken to identify the nature of this synergistic effect.

Experimental Section

Catalyst synthesis: RuNPs@SILP were prepared as previously reported.^[3b] Full experimental and characterization data are provided in the Supporting Information.

Batch conditions: In a typical experiment, RuNPs@SILP (75 mg, 0.0024 mmol Ru), phenol (6.0 mmol, 2500 equiv), and decalin (1 mL) were combined in a glass insert and placed in a high-pressure

autoclave. After purging the autoclave with H₂, the reaction mixture was stirred at 150 °C in an aluminum heating block under 120 bar H₂ (pressurized to 100 bar H₂ at RT). Once the reaction was finished, the reactor was cooled in an ice bath, carefully vented, and the reaction mixture was analyzed by GC using hexadecane as an internal standard.

Continuous flow conditions: A 70 mm CatCart was filled with RuNPs@SILP-1.00 (540 mg, 0.0173 mmol Ru) and placed into a flow reactor (H-Cube Pro). Prior to catalysis, the catalyst was heated at 100 °C under a flow of decalin (0.3 mL min⁻¹) and H₂ (80 bar; gas flow rate under standard conditions = 60 NmL min⁻¹) for 30 min. The substrate solution (0.05 M phenol in decalin) was introduced into the system with a flow of H₂ (80 bar) and the reaction parameters (temperature = 110–150 °C, substrate flow = 0.3–0.9 mL min⁻¹, H₂ flow rate = 60–90 NmL min⁻¹) were varied. The system was allowed to equilibrate under the desired reaction conditions for 20 min before approximately 6 mL of reaction solution was collected. The reaction mixture was analyzed by GC using hexadecane as an internal standard.

Acknowledgements

This work was performed as a part of the Cluster of Excellence “Tailor-Made Fuels from Biomass”, which is funded by the Excellence Initiative of the German federal and state governments to promote science and research at German universities. Additional support by the the European Union (Marie Curie ITN “SuBiCat” PITN-GA-2013–607044) is gratefully acknowledged. The authors would like to thank Karl-Josef Vaeßen (ITMC, RWTH Aachen University) for N_{2(g)} adsorption measurements, Bernd Spliethoff and Hans-Josef Bongard (Max-Planck-Institut für Kohlenforschung) for TEM and STEM analyses, and Dr. Nils Theysen (Max-Planck-Institut für Kohlenforschung) for his generous support. K.L.L. would like to thank Deutscher Akademischer Austausch Dienst (DAAD) for financial support. P.M. would like to thank the Alexander von Humboldt Foundation for funding.

Keywords: bifunctional catalysts · biomass conversion · kinetics · lignin · ruthenium

How to cite: *Angew. Chem. Int. Ed.* **2015**, *54*, 15750–15755
Angew. Chem. **2015**, *127*, 15976–15981

- [1] a) A. Corma, S. Iborra, A. Velty, *Chem. Rev.* **2007**, *107*, 2411–2502; b) M. J. Climent, A. Corma, S. Iborra, *Green Chem.* **2014**, *16*, 516–547; c) J. N. Chheda, G. W. Huber, J. A. Dumesic, *Angew. Chem. Int. Ed.* **2007**, *46*, 7164–7183; *Angew. Chem.* **2007**, *119*, 7298–7318; d) D. M. Alonso, J. Q. Bond, J. A. Dumesic, *Green Chem.* **2010**, *12*, 1493–1513; e) M. Besson, P. Gallezot, C. Pinel, *Chem. Rev.* **2014**, *114*, 1827–1870; f) T. vom Stein, J. Klankermayer, W. Leitner, in *Catalysis for the Conversion of Biomass and its Derivatives* (Eds.: M. Behrens, A. K. Datye), epubli, Berlin, **2013**, pp. 411–434.
- [2] a) F. M. A. Geilen, B. Engendahl, A. Harwardt, W. Marquardt, J. Klankermayer, W. Leitner, *Angew. Chem. Int. Ed.* **2010**, *49*, 5510–5514; *Angew. Chem.* **2010**, *122*, 5642–5646; b) F. M. A. Geilen, B. Engendahl, M. Holscher, J. Klankermayer, W. Leitner, *J. Am. Chem. Soc.* **2011**, *133*, 14349–14358.
- [3] a) J. Julis, W. Leitner, *Angew. Chem. Int. Ed.* **2012**, *51*, 8615–8619; *Angew. Chem.* **2012**, *124*, 8743–8747; b) K. L. Luska, J.

- Julis, E. Stavitski, D. N. Zakharov, A. Adams, W. Leitner, *Chem. Sci.* **2014**, *5*, 4895–4905.
- [4] A. M. Ruppert, K. Weinberg, R. Palkovits, *Angew. Chem. Int. Ed.* **2012**, *51*, 2564–2601; *Angew. Chem.* **2012**, *124*, 2614–2654.
- [5] a) J. Zakzeski, P. C. A. Bruijninx, A. L. Jongerius, B. M. Weckhuysen, *Chem. Rev.* **2010**, *110*, 3552–3599; b) C. P. Xu, R. A. D. Arancon, J. Labidi, R. Luque, *Chem. Soc. Rev.* **2014**, *43*, 7485–7500.
- [6] a) J. M. Nichols, L. M. Bishop, R. G. Bergman, J. A. Ellman, *J. Am. Chem. Soc.* **2010**, *132*, 12554–12555; b) A. G. Sergeev, J. F. Hartwig, *Science* **2011**, *332*, 439–443; c) S. Kusumoto, K. Nozaki, *Nat. Commun.* **2015**, *6*, 6296; d) T. vom Stein, T. Weigand, C. Merckens, J. Klankermayer, W. Leitner, *ChemCatChem* **2013**, *5*, 439–441; e) T. vom Stein, T. den Hartog, J. Buendia, S. Stoychev, J. Mottweiler, C. Bolm, J. Klankermayer, W. Leitner, *Angew. Chem. Int. Ed.* **2015**, *54*, 5859–5863; *Angew. Chem.* **2015**, *127*, 5957–5961; f) P. J. Deuss, M. Scott, F. Tran, N. J. Westwood, J. G. de Vries, K. Barta, *J. Am. Chem. Soc.* **2015**, *137*, 7456–7467.
- [7] a) X. Y. Wang, R. Rinaldi, *Angew. Chem. Int. Ed.* **2013**, *52*, 11499–11503; *Angew. Chem.* **2013**, *125*, 11713–11717; b) P. Ferrini, R. Rinaldi, *Angew. Chem. Int. Ed.* **2014**, *53*, 8634–8639; *Angew. Chem.* **2014**, *126*, 8778–8783; c) Y. L. Ren, M. J. Yan, J. J. Wang, Z. C. Zhang, K. S. Yao, *Angew. Chem. Int. Ed.* **2013**, *52*, 12674–12678; *Angew. Chem.* **2013**, *125*, 12906–12910; d) S. Van den Bosch, W. Schutyser, R. Vanholme, T. Driessen, S. F. Koelewijn, T. Renders, B. De Meester, W. J. J. Huijgen, W. Dehaen, C. M. Courtin, B. Lagrain, W. Boerjan, B. F. Sels, *Energy Environ. Sci.* **2015**, *8*, 1748–1763; e) R. Ma, K. Cui, L. Yang, X. L. Ma, Y. D. Li, *Chem. Commun.* **2015**, *51*, 10299–10301.
- [8] a) H. M. Wang, J. Male, Y. Wang, *ACS Catal.* **2013**, *3*, 1047–1070; b) D. A. Ruddy, J. A. Schaidle, J. R. Ferrell, J. Wang, L. Moens, J. E. Hensley, *Green Chem.* **2014**, *16*, 454–490.
- [9] D. Fengel, G. Wegener, *Wood: Chemistry, Ultrastructure, Reactions*, Walter de Gruyter, Berlin, **1989**.
- [10] a) C. Zhao, Y. Kou, A. A. Lemonidou, X. B. Li, J. A. Lercher, *Angew. Chem. Int. Ed.* **2009**, *48*, 3987–3990; *Angew. Chem.* **2009**, *121*, 4047–4050; b) C. Zhao, Y. Kou, A. A. Lemonidou, X. B. Li, J. A. Lercher, *Chem. Commun.* **2010**, *46*, 412–414; c) N. Yan, Y. A. Yuan, R. Dykeman, Y. A. Kou, P. J. Dyson, *Angew. Chem. Int. Ed.* **2010**, *49*, 5549–5553; *Angew. Chem.* **2010**, *122*, 5681–5685; d) D. Y. Hong, S. J. Miller, P. K. Agrawal, C. W. Jones, *Chem. Commun.* **2010**, *46*, 1038–1040; e) W. Zhang, J. Z. Chen, R. L. Liu, S. P. Wang, L. M. Chen, K. G. Li, *ACS Sustainable Chem. Eng.* **2014**, *2*, 683–691; f) Y. Nakagawa, M. Ishikawa, M. Tamura, K. Tomishige, *Green Chem.* **2014**, *16*, 2197–2203; g) Y. B. Huang, L. Yan, M. Y. Chen, Q. X. Guo, Y. Fu, *Green Chem.* **2015**, *17*, 3010–3017; h) L. Wang, J. Zhang, X. F. Yi, A. M. Zheng, F. Deng, C. Y. Chen, Y. Y. Ji, F. J. Liu, X. J. Meng, F. S. Xiao, *ACS Catal.* **2015**, *5*, 2727–2734; i) C. R. Lee, J. S. Yoon, Y. W. Suh, J. W. Choi, J. M. Ha, D. J. Suh, Y. K. Park, *Catal. Commun.* **2012**, *17*, 54–58.
- [11] K. L. Luska, P. Migowski, W. Leitner, *Green Chem.* **2015**, *17*, 3195–3206.
- [12] a) B. Karimi, M. Vafaezadeh, *Chem. Commun.* **2012**, *48*, 3327–3329; b) D. Elhamifar, B. Karimi, A. Moradi, J. Rastegar, *ChemPlusChem* **2014**, *79*, 1147–1152.
- [13] R. Fehrmann, A. Riisager, M. Haumann, *Supported Ionic Liquids: Fundamentals and Applications*, Wiley-VCH, Weinheim, **2014**.
- [14] a) M. A. Gelesky, S. S. X. Chiaro, F. A. Pavan, J. H. Z. dos Santos, J. Dupont, *Dalton Trans.* **2007**, 5549–5553; b) L. Luza, A. Gual, D. Eberhardt, S. R. Teixeira, S. S. X. Chiaro, J. Dupont, *ChemCatChem* **2013**, *5*, 2471–2478; c) N. Karbass, V. Sans, E. Garcia-Verdugo, M. I. Burguete, S. V. Luis, *Chem. Commun.* **2006**, 3095–3097; d) M. I. Burguete, E. Garcia-Verdugo, S. V. Luis, J. A. Restrepo, *Phys. Chem. Chem. Phys.* **2011**, *13*, 14831–14838; e) V. Sans, F. Gelat, N. Karbass, M. I. Burguete, E. Garcia-Verdugo, S. V. Luis, *Adv. Synth. Catal.* **2010**, *352*, 3013–3021.
- [15] S. Winterle, M. A. Liauw, *Chem. Ing. Tech.* **2010**, *82*, 1211–1214.
- [16] S. Miao, Z. Liu, B. Han, J. Huang, Z. Sun, J. Zhang, T. Jiang, *Angew. Chem. Int. Ed.* **2006**, *45*, 266–269; *Angew. Chem.* **2006**, *118*, 272–275.

Received: September 11, 2015

Published online: November 5, 2015